Dalton Transactions

Accepted Manuscript

This is an *Accepted Manuscript*, which has been through the Royal Society of Chemistry peer review process and has been accepted for publication.

Accepted Manuscripts are published online shortly after acceptance, before technical editing, formatting and proof reading. Using this free service, authors can make their results available to the community, in citable form, before we publish the edited article. We will replace this *Accepted Manuscript* with the edited and formatted *Advance Article* as soon as it is available.

You can find more information about *Accepted Manuscripts* in the Information for Authors.

ROYAL SOCIETY OF CHEMISTRY

www.rsc.org/dalton

Two isoreticular metal–organic frameworks with $CdSO_4$-like topology: selective gas sorption and drug delivery

Jian-Qiang Liu[a*], Jian Wu[b], Zhen-Bin Jia[a], Hong-Lang Chen[a], Qing-Lin Li[a], Hiroshi Sakiyama[c], Thereza A. Soares[d*], Ren-Fei[e]* Carole Daiguebonne[f], Olivier Guillou[f*], Ng Seik Weng[g]

[a] *School of Pharmacy, Guangdong Medical College, Dongguan, 523808, P. R. China*

[b] *Guangxi Key Laboratory of Chemistry and Engineering of Forest Products, Guangxi University for Nationalities, College of Chemistry and Chemical Engineering, Nanning, Guangxi 530006, China*

[c]*Department of Material and Biological Chemistry, Faculty of Science, Yamagata University, Kojirakawa, Yamagata 990-8560, Japan*

[d]*Departament de Fundamental Chemistry, Universidade Federal de Pernambuco, Cidade Universit_aria, Recife 50740-560, Brazil*

[e]*Department of Pharmacy, Nanfang Hospital, Southern Medical University, Guangzhou 510515, China*

[f] *INSA, UMR 6226 "Institut des Sciences Chimiques de Rennes", F-35708 Rennes, France*

[g]*Department of Chemistry University of Malaya 50603 Kuala Lumpur Malaysia and Chemistry Department King Abdulaziz University, PO Box 80203 Jeddah, Saudi Arabia*

Abstract:

Two isoreticular metal–organic frameworks with chemical formulae $[Cu(L)(4,4'\text{-bipy})(H_2O)]_n \cdot 1.5nCH_3CN$ (**1**) and $[Cu(L)(4,4'\text{-bipy})(H_2O)]_n \cdot 4nH_2O$ (**2**) (H_2L= diphenylmethane-4,4'-dicarboxylic acid) were synthesized and structurally characterized. They show **$CdSO_4$** ($6^5.8$) net and have obvious 1-D channel that spread along the crystallographic *c* axis. More importantly, **1** shows high selectivity for H_2 over N_2 and CO_2 at low pressure, which could be confirmed via computational calculations using Connolly algorithm to reveals the size and shape of accessible voids. The incorporation of the drug 5-fluorouracil (5-FU) into the desolvated **1** was around 27.5 wt% per gram of dehydrated **1**. 5-FU is released in a highly controlled and progressive fashion with 61 % of the drug released after 95 hours. In addition, we have applied molecular docking calculations to investigate the preferred conformation of 5-FU molecules upon binding to MOF **1**. These calculations provide a structural basis to explain the 5-FU release from MOF **1**.

Introduction

Metal–organic frameworks (MOFs) have drawn considerable attention in recent years

and have been evaluated for their promising applications in delivery and gas technology.[1-2] Particularly, MOFs as drug-delivery vehicles are highly desirable in view of their large loadings of drugs, and biodegradability.[3] Férey and his co-workers reported an example of non-toxic porous iron(III)-based MOFs, which shows nano-carriers for controlled delivery of several anti-tumoural and retroviral drugs.[3d] Recently, ZIF-8 has been demonstrated to be an outstanding metal imidazolate framework showing high porosity and exceptional stability and also exhibiting interesting properties for a carrier.[4] Some a few of MOFs allow high amounts of drugs to be loaded, with a complete delivery time ranging from 6 to 30 days.[5-10]

Recently, flexible dicarboxylate derivatives have been developed to assemble MOFs, which shows intrinsic charming topologies and excellent gas absorption capacity using the advantage of their active metal centers and large permanent prosity.[11] We have been interested in the syntheses and characterization of MOFs containing the series of organic linkers of 4,4'-oxybis(benzoic acid) (H_2oba), 1,2-bis(4-carboxy-phenoxy)ethane(H_2bce) and 1,3-bis(4-carboxy-phenoxy)propane (H_2bcp). Among the three types of flexible dicarboxylate ligands, the segment of –O-X-O- chains are different with respect with the relative orientation of CH_2 groups.[12] However, the control of product architectures still remains a major challenge in this field due to some uncertain factors.[13] Herein, we chose a new flexible ligand L to construct nonporous MOFs. Fortunately, two isoreticular metal–organic frameworks of $[Cu(L)(4,4'\text{-bipy})(H_2O)]_n\cdot 1.5nCH_3CN$ (**1**) and $[Cu(L)(4,4'\text{-bipy})(H_2O)]_n\cdot 4nH_2O$ (**2**) have been prepared. Their drug load and release capacity using an anticancer drug of 5-fluorouracil (5-FU), as a model was evaluated. In addition, we have investigated the preferred conformation of 5-FU upon binding to MOF **1** when another 5-FU molecule is already bound in the pore. **1** shows high selectivity for H_2 over N_2 and CO_2 at low pressure, which is also corroborated by molecular surface calculations based on Connolly algorithm[14].

Materials and Method

All reagents were purchased from commercial sources and used as received. IR spectra were recorded with a Perkin–Elmer Spectrum One spectrometer in the region 4000–400cm^{-1} using KBr pellets. TGA were carried out with a Metter–Toledo TA 50 under dry dinitrogen flux (60mL.min^{-1}) at a heating rate of 5°C min^{-1}. X-ray powder

diffraction (XRPD) data were recorded on a Rigaku RU200 diffractometer at 60KV, 300mA for *Cu* K_α radiation (λ = 1.5406 Å), with a scan speed of 2 °C/min and a step size of 0.02° in 2θ. Magnetic susceptibility data of powdered samples restrained in parafilm were measured on Oxford Maglab 2000 magnetic measurement system in the temperature range 300–1.8 K and at field of 1KOe. All the gas sorption isotherms were measured by using a ASAP 2020M adsorption equipment.

X-ray Crystallography

Single crystal X-ray diffraction analyses of the two compounds were carried out on a *Bruker SMART APEX II CCD* diffractometer equipped with a graphite monochromated Mo*K*α radiation (λ = 0.71073 Å) by using ϕ/ω scan technique at room temperature. The intensities were corrected for Lorentz and polarization effects as well as for empirical absorption based on multi-scan techniques; all structures were solved by direct methods and refined by full-matrix least-squares fitting on F^2 by SHELX-97.[15] Absorption corrections were applied by using multi-scan program SADABS.[16] Non-hydrogen atoms were refined anisotropically. The hydrogen atoms of organic ligands were placed in calculated positions and refined using a riding on attached atoms with isotropic thermal parameters 1.2 times those of their carrier atoms. The water hydrogen atoms were located from difference maps and refined with isotropic thermal parameters 1.5 times those of their carrier atoms. The guest solvent molecules in the crystal and they are impossible to refine using conventional discrete atom models, the SQUEEZE subroutine of the PLATON software suite was applied to remove the scattering from the highly disordered solvent molecules, and sets of solvent-free diffraction intensities were generated. Three acetonitrile (a C_2H_3N has 24 electrons) molecules are presumed to reside in each of the twi 301Å^3 voids in **1**. Eight water molecules are presumed to reside in each of the two 319 Å^3 voids in **2**. The formula units of **1-2** were arrived at through a combination of elemental analyses, infrared and thermogravimetric characterization. The more detail information are listed in the cif files. The Cu(II) and O1w atoms have been refined as two equal positions (the copper atom and water molecule were allowed to refine off the center-of-inversion) in **2**. Selected bond distances and bond angles are listed in Table 2. **CCDC**: 1001340-1001341.

Synthesis of the complexes

$[Cu(L)(4,4'\text{-bipy})(H_2O)]_n \cdot 1.5nCH_3CN$ (**1**)

A mixture of $Cu(NO_3)_2 \cdot 3H_2O$ (0.024g, 0.1mmol), H_2L (0.032 g, 0.1mmol), 4,4'-bipy (0.012 g, 0.1mmol), CH_3OH (2 mL), CH_3CN (5 mL) and deionised water (5mL) was stirred for 30min in air. The pH of the resulting solution was adjusted to 7 using dilute NaOH (0.1mol/L) and kept at 120 °C for 72h at oven, and then cooled down to 25 °C. The resulting crystals formed were filtered off, washed with water and dried in air. $C_{28}H_{24.5}CuN_{3.5}O_5$. Calcd: C, 60.75; H, 4.46; N, 8.86. Found C, 60.98.; H, 4.52; N, 8.71. **IR** (KBr, cm^{-1}): 3402(vs); 3041(w); 2916(w); 1611(vs); 1541(s); 1391(vs); 1195(s); 795(vs); 762(s).

$[Cu(L)(4,4'\text{-bipy})(H_2O)]_n \cdot 4nH_2O$ (**2**)

The synthesis procedure of **2** is similar to that for **1**, except that the synthetic temperature was kept at 105 °C. $C_{25}H_{28}CuN_2O_9$. Calcd: C, 53.24; H, 5.00; N, 4.96. Found C, 52.97; H, 5.04; N, 4.98. **IR** (KBr, cm^{-1}): 3339(vs); 3139(vs); 2938(m); 1592(vs); 1352(vs); 1093(vs); 999(m); 847(vs); 779(vs).

Computational Procedure

Molecular docking calculations were performed for four tautomeric forms of 5-FU (Figure 7) and the metal-organic framework of $[Cu(L)(4,4'\text{-bipy})(H_2O)]_n \cdot 1.5nCH_3CN$ (**1**) using a hybrid search method based on the Lamarckian genetic algorithm (LGA) implemented in the AutoDock4 software.[17] Degrees of translation, and orientation of 5-FU were treated as fully flexible with respect to the framework **1** structure, which was kept rigid. Each sampled conformation was evaluated and ranked according to an molecular mechanics empirical energy function.[18] Grid maps with 126 X 126 X 126 points of dimension were calculated using AutoGrid4.[19] Coarse (grid-point spacing of 0.30 Å) and fine (grid-point spacing of 0.14 Å) sets of grid maps were used during the docking simulations in order to sample the entire MOF **1** structure and to improve the accuracy of energy estimates for host-guest interactions. Atomic charges for MOF **1** and 5-FU tautomers were assigned according to Amber86 force field,[20] ensuring that all residues have integer charges. The Amber86 atom types were assigned to all atoms. The LGA parameters used during the conformational search were: an initial population of 50 random individuals, a maximum number of 1.5 x 10^6 energy evaluations, a maximum number of 27000 generations, and mutation and crossover rates of 0.02 and 0.08,

respectively. An optional elitism parameter equal to 1 was applied. A maximum of 300 iterations per local search was allowed. The lowest energy docked conformations were sorted in order of increasing energy and the root-mean-squared deviation (RMSD) of each conformation was calculated and compared in order to cluster together conformations with a RMSD smaller than 2.0 Å. A detailed description of the LGA parameters and procedures employed here can be found elsewhere[21]. Previous applications of the molecular docking methodology to predict the binding conformation of drug-MOF complexes have also been reported[22].

Results and Discussion

Syntheses of the MOFs

Two isoreticular metal–organic frameworks **1** and **2** were obtained *via* the solvothermal reaction of $Cu(NO_3)_2 \cdot 3H_2O$ with L in CH_3CN under the same reaction conditions described, except for the reaction temperature of the reactant used. While **1** was obtained under 120 °C, **2** was prepared *via* the same solvothermal reaction, but at a lower reaction temperature, 105°C. The reaction used of the same reactant process employed for the synthesis of **2** under 120 °C, which led to the formation of powder. Cheetham and his co-worker found less water for complexes formed at higher temperatures is likely driven by the increased entropic contribution associated with releasing water from a confined state in these solids to a liquid state[13f-g]. The pH values of the reaction solutions does not play a role key in determining the final products, although we have tried to adjust the pH (such as 6 and 7.5) at different degrees.

$[Cu(L)(4,4'\text{-bipy})(H_2O)]_n \cdot 1.5nCH_3CN$ (**1**)

The asymmetric unit of **1** has one Cu(II) center, one doubly deprotonated L ligand, one 4,4'-bipy molecule, one coordinated water molecule and 1.5 CH_3CN free molecules. The Cu(II) atom shows a square base pyramidal $[CuN_2O_3]$ coordination geometry (Fig. 1a), where the N atoms belong to two different 4,4'-bipy linkers and the two O atoms (O1and O3) from different L ligands. The vertex position is occupied by the coordinated water molecule (O1W). Adjacent Cu(II) atoms bind to each L anion through carboxylate oxygen atoms on the same side of the orientation, so that neutral zigzag 1-D $[Cu(L)]_n$ chains with a Cu–Cu distance of 13.88 Å are formed (Fig. S1). Mutually orthogonal sets the $[Cu(4,4'\text{-bipy})]_n$ chains run parallel to the a and c crystal directions(Fig. S2). The two

types of chains in **1** are in turn strutted each other, resulting in a 3D 4-connected **$CdSO_4$** (circuit symbol ($6^5.8$) or Schläflinotation ($6.6.6.6.6_2.\infty$)) topology framework (Fig.2, Fig. 3 and see ESI for the detailed topological information)[23,24]. This MOF is a microporous framework, and the pore openings as viewed along the c-axis are rhombic in shape and have dimensions of about 10.7×13.8 $Å^2$ (excluding the van der Waals radii of the atoms). Moreover, such arrangement makes **1** become a 3D continuous intersecting channel system (Fig. 2b) with highly solvent accessible voids of 23.6%.

$[Cu(L)(4,4'\text{-bipy})(H_2O)]_n \cdot 4nH_2O$ (**2**)

The asymmetric unit of **2** has one Cu(II) center, one doubly deprotonated L ligand, one 4,4'-bipy molecule, one coordinated water molecule and 4 free water molecules. The Cu(II) exhibits square-pyramidal geometry with vertex position is occupied by one water molecule(Fig.1b). The coordinated mode and arrangement of L and 4,4'-bipy are very similar with that of **1** (Fig.S3 and S4). So, a $[Cu(L)(H_2O)]_n$ chain is also constructed parallel the *ac*-plane (Fig.S3). Thus, the compounds **1** and **2** are isoreticular metal–organic frameworks. The volume of the solvent channels comprises 23% of the total unit cell volume.

From the above discussion, the two coordination networks are fairly rigid - the 4,4'-bipyridines link the metal centers to form a layer. Then, the V-shaped carboxylates link the layers into a 3D network. Although the organic linkers containing L and 4,4'-bipy have the same coordinated modes, the Cu...Cu distances are different (13.8 Å for **1** and 5.5 Å for **2**) due to the different bridging modes of water molecule. But they have the similar frameworks because of the same linkage of 4,4'-bipy layer. Moreover, from the calculation values of the solvent channels, **1** and **2** also have the same void, which can be proved by latter molecular docking calculations.

Thermogravimetric Analyses and XRPD

To study the stabilities of the polymers, thermogravimetric analyses (TGA) of complexes **1-2** were performed (Fig. S5). The compound **1** shows two weight loss steps. The first weight loss begins at 80°C and is completed at 180°C. The observed weight loss of 12.3% is corresponding to the loss of 1.5 CH_3CN and coordinated water molecule (calcd 11.5%). The second weight loss occurs latterly, and can be attributed to the elimination of bipy and L ligands (obsd: 72.2%; calcd 71.7%). The compound **2** also has

two observed weight loss. First weight loss of 16.1% is corresponding to the loss of the crystallization water and coordinated water molecules (calcd 16.0%). A gradual weight loss from 280 °C indicates that the complex decomposes continuously when the temperature is rising up.

Additionally, to confirm the phase purity of compounds, the original samples were characterized by X-ray powder diffraction (XRPD) at room temperature. The patterns that were simulated from the single-crystal X-ray data of compounds were in agreement with those that were observed (Fig. S6). The powder XRD pattern of MOFs samples shows small shifts in the peak positions and some peaks are also missing. This suggests minor rearrangements of atoms upon replacement of guest molecules.

The $\chi_m T$ value was 0.68 cm^3 K mol^{-1} at 300 K in **1** (Fig. 4a), and this is larger than the spin only value (0.38 cm^3 K mol^{-1}) for the S = 1/2 state. A similar phenomenon is documented in the case of $[CuL](Cl_2)\cdot 2H_2O$ (L = 6,13-bis(dodecylaminomethylidene)-1,4,8,11-tetrazacyclotetradeca- 4,7,11,14-tetraene) complex, the $\chi_m T$ value of 0.75 cm^3 K mol^{-1} for one Cu(II) atom is observed at a room temperature.[25m] When decreasing the temperature, the $\chi_m T$ decreases monotonously (0.40 cm^3 K mol^{-1} at ~20 K), and drops to a minimum (0.27 cm^3 K mol^{-1} at 2 K). If the data was analyzed based on the Lines' simple-cubic-lattice equation,[25a] the parameters were obtained as follows: $J = -0.42$ cm^{-1}, g = 2.07 cm^{-1}, and TIP = 1.005 × 10^{-6} cm^3 mol^{-1}, where TIP represents temperature-independent paramagnetism caused by a coupling with the excited states. The temperature-independent paramagnetism (TIP) is typically of order 10^{-6} for Cu(II) complexes.[25j] Temperature Independent Paramagnetism is of importance in the study of metal complexes from two points of view. First, because it may need to be corrected for when calculating μ_{eff} values, and secondly because it can be used in complexes to obtain an estimate of the ligand field parameter for d^n systems. Thus, the TIP value is related to the framework in some degree. TIP is much larger than the mononuclear copper(II) complex, but it may due to the 3D structure. The decrease in $\chi_m T$ from 300 K to ~20 K is mainly due to the TIP, and the drop below 20 K is due to the antiferromagnetic interactions. In conclusion, the antiferromagnetic interaction is no doubt very small.[25a]

The $\chi_m T$ value was 0.225 cm^3 K mol^{-1} at 300 K in **2** (Fig. 4b), and this is smaller than the spin only value (0.38 cm^3 K mol^{-1}) for the S = 1/2 state, suggesting an

antiferromagnetic interaction. A similar value of $\chi_m T$ at room temperature are 0.68 cm^3 K mol^{-1} was observed at a complex of $(Bu_4N)_2[Cu(dmso)_2\{Cu(dnopba)(dmso)\}_2]$, which is well below the expected one for three magnetically isolated spin doublets ($\chi_m T$ = 1.24 cm^3 K mol^{-1}).[25k] When decreasing the temperature, the $\chi_m T$ decreases gradually till at around 80 K (0.055 cm^3 K mol^{-1} at ~80 K), and slightly decreases to the minimum (0.036 cm^3 K mol^{-1} at 2 K). In the χ_m versus T plot, χ_m shows a maximum at around 200 K, but it increases below 70 K. The observed data could not be well simulated based on models, including cubic lattice model, quadratic layer model, linear chain model; however, the decrease in $\chi_m T$ from 300 K to ~80 K must be due to an antiferromagenetic interaction, and this seems to be consistent with the maximum in χ_m at ~200 K. The data could be fitted with the parameters, $J = -250$ cm^{-1}, $zJ' = -250$ cm^{-1}, $g = 2.04$ cm^{-1}.

Although compounds reported in this paper (**1-2)** show similar antiferromagnetic behavior, the observed $\chi_m T$ values are different. In compound **1,** each Cu(II) ion is linked to four neighboring Cu(II) ions, by two 4,4'-bipy bridges with a Cu…Cu distance of 13.88 Å and two L bridges with Cu…Cu distance of 11.17 Å. Since these bridges should pass weak antiferromagnetic interactions with similar amplitudes.[25] It has already been established that the coupling in Cu(II) centers bridged by only long organic linkers is generally very weak.[25i] The obtained value J is smaller than values reported in the related literature.[25] This behavior could be rationalized on the basis of the existence of only two bridging ligands per copper pair and larger separations in **1** as was discussed in detail above (description of the structure). In compounds **2**, the H_2O fixes the copper atoms in a related flexible molecular frame and makes a binuclear subunit. Considering magneto-structural correlations,[25] magnetic behavior of Cu(II) complexes with hydroxo/alkoxo bridged oxygen atoms is highly dependent on the Cu-O-Cu bridge angles and usually display antiferromagnetic character when the Cu-O-Cu angles exceed the value of 98°,[25g] this coordination polymer of **2** presents the Cu-O-Cu bridge angle of 174.8(2)°. Furthermore, the obtained J value of -250 cm^{-1} is consistent with the typical values in the range of -140 to -270 cm^{-1} for similar binuclear compounds.[25i]

To examine porosity, **1** was activated at 100 °C for 10 h under vacuum (Fig.S6). The N_2 and CO_2 sorption isotherms were performed at 77 and 195 K; the maximum N_2 and CO_2 uptakes are 44.0 and 86.5 cm^3 g^{-1}, respectively (Fig. 5). The hysteresis character

may come from the hindered escape of adsorbed gases in the pores during the desorption process for the kinetic diameters of N_2 (3.64 Å) and CO_2 (3.30 Å) which are close to the pore sizes of **1**; therefore, it shows a more obvious hysteresis feature for N_2 desorption due to its larger kinetic diameter. This is also the reason for the higher uptakes of CO_2 than N_2 usually observed in a microporous MOF. More interestingly, at 77 K and ambient pressure, **1** exhibits much higher sorption selectivity for H_2 than CO_2 and N_2. As shown in Fig. 5, **1** adsorbs 93.3 $cm^3.g^{-1}$ H_2 at 1 atm, which is moderately high and comparable to values in recently reported porous MOFs.[26] The observed hysteresis loop between the adsorption and desorption processes indicates the global cooperative movement of the frameworks in the entire crystal of **1**. Similar adsorption isotherms of H_2, N_2 and CO_2 were observed for others MOFs, which indicates that the intrinsic interframework interaction rather than the specific host-guest interaction fairly contributes to the gate-opening behavior[26]. High selectivity and good sorption capacity are crucial parameters for a MOF as a gas separation material.

The computational method, based on Connolly's algorithm has already been described and successfully used elsewhere[14,27]. Thanks to this method, porosity profile can be calculated on the basis of the crystal structure. The compound exhibits quite sizeable potential porosity. The channels that spread along the c axis can host guest molecules that present a kinetic radius as large as 2.1Å (Figure S7). Smaller channels spread along the *a* axis. The potential porosity has been calculated for several probe sphere radii that correspond to different guest molecules kinetic radii (see Table S1).[27e] Difference between experimental and simulated values can be attributed to an incomplete de-solvation and/or a partial collapse of the crystal structure upon the de-solvation process.

Before its use as a drug delivery carrier, polymer **1** was activated. Then, adsorption of anticancer 5-FU was carried out by impregnating **1** under stirring in 5-FU containing ethanol solutions. As evidenced by PXRD, 5-FU containing sample maintains its crystallinity (Fig.S6). Incorporation of the drug molecule during adsorption process has been confirmed by Fourier transformed infrared spectroscopy (FTIR) (Figure S8). The characteristic peaks of 5-FU observed at 1724, and 1248 cm^{-1} can be attributed to the stretching vibration of C=O, and C–N groups, respectively. The absorption bands of C–F

deformations were also discovered in the 820–550 cm^{-1} regions. The absorption band at about 1240 cm^{-1} may be due to fluorine atom on the ring. Furthermore, the shift of the *v*(C=O) band of the carboxylic group of 5-FU from 1677 to 1699 cm^{-1} correlated to those of the vibrational band *v*(O-H) of the polymer **1** from 3448 to 3415 cm^{-1}, indicates the formation of a hydrogen bond between the carboxylic group of 5-FU and the hydroxyl group of water molecule of **1**.[3d,28]

HPLC has been used to determine the effective **1** storage capacity. To reach a maximal drug loading, 5-FU to porous solid, relative ratio and contact time were tested (Table S2). It was observed that adsorbed amount of 5-FU increased with initial 5-FU/material ratio expressed in weight and optimal value (2:1) corresponding to maximum solubility of 5-FU in ethanol. The contact time was also important. The maximum adsorption was obtained after 5 days. Chemical analysis indicates that desolvated **1** adsorbs 0.275 g of 5-FU g^{-1} per gram of desolvated **1**, which is little lower than the 5-FU loading in the Cu(pi)-PEG5k reported by Zhou and co-workers.[6]

Drug-release experiments were carried out by dialyzing the drug-loaded **1** against phosphate buffered saline (PBS) buffer solution (pH 7.4) at room temperature and measured by HPLC. A progressive release was observed with no "burst effect" (the burst effect is normally taken as the high release rates that can be reached in the initial stages after activation and is often regarded as a negative consequence of creating long-term controlled release devices)[29]. The delivery of 5-FU occurred within 95hs and 61% of the loaded drug was released (Fig. 6). Three stages related to the drug release could be distinguished. Around 21% of the loaded drug was released in the first stage (11 h) and 51% was released in the later two stages. As mentioned in the structural analysis, one size of nanoscale cage exists in **1** and the window is larger (10.5 Å x 10.7 Å) than the size of the drug molecule (5.3 Å × 5.0 Å). For those drug molecules approaching the pore walls, the interaction between Lewis acid sites in **1** and base sites in 5-FU may lead to this relatively slow release. XRPD performed before and after 5-FU release shows that the crystal structures are similar with each other (Fig.S6).

Molecular docking calculations[22] were performed for the diketo and dienol forms of 5-FU into frameworks **1** and **2**, and for the four tautomeric forms of 5-FU into framework **1** (Figure 7). 5-FU fits compactly into the framework pores where it interacts mostly with

the metal and the carboxylate groups of the ligand (Figure 8a). In framework **1**, ligand atoms (oxygen and nitrogen) and the metal Cu(II) surround the structural water molecules. The clustering of highly charged atoms around these water molecules hinders interactions between the latter and 5-FU. Indeed, the molecular docking calculations show that 5-FU binds analogously to both frameworks regardless of the presence of structural water molecules. This is consistent with the fact that the dimensions and chemical environment of the pore nearly identical for **1** and **2** (Figure S9). The predominant conformations for the four tautomeric forms of 5-FU exhibit hydrogen bonds between the protonated heterocyclic nitrogen and/or hydroxyl groups in 5-FU and the carboxylate group in the ligand (Figure 8b). In addition, we have investigated the preferred conformation of 5-FU (diketo form) upon binding to MOF **1** when another 5-FU molecule is already bound in the pore. The small size of the pore does not allow the π stacking of two 5-FU molecules. Instead, two 5-FU molecules interact with each other in a linear fashion along the pore channel *via* hydrogen bonds (Figure 9). In this conformation, two 5-FU molecules occupy a surface of ca. 240 $Å^2$ within the MOF pore. The predominant conformations for single or multiple docked molecules favor hydrogen bond or electrostatic interactions with the charged regions surrounding the Cu(II) (Figure 9).

Conclusion

Two isoreticular metal–organic frameworks showing **$CdSO_4$** ($6^5.8$) topology have been rational designed using two different linkages. **1** shows high selectivity for H_2 over N_2 and CO_2 at low pressure. Moreover, **1** has been evaluated as potential carrier for the adsorption and delivery of anticancer 5-FU. Our results show that **1** adsorbs 0.275 g of 5-FU g^{-1} per gram of desolvated **1**, with a progressive release of the drug without any "burst effect". The kinetics of 5-FU follows well-defined pattern: 21% of the loaded drug is released in the first 11 h, and 51% is released in two slower stages. Molecular docking calculations suggest that 5-FU molecules fit snugly into the pores of **1**, therefore providing an explanation for the slow release of 5-FU from **1**. It is suggested interactions between Lewis acid sites in **1** and base sites in 5-FU may lead to the slow release of 5-FU.

Acknowledgments

This work was partially supported by the Grants from the National Natural Science Foundation of

China (21201044), Natural Science Foundation of Guangdong Province(S2012040007835), Foundation for Distinguished Young Talents in Higher Education of Guangdong Province (LYM11069), Technologies R & D program of Zhanjiang (2011C3108013 and 2012C3106016), Guangxi University for Nationalities (2011DQ022), Training plan of Guangdong Province outstanding young teachers in Higher Education Institutions (Grant No.YQ2013084), Science & Technology Innovation Fund of Guangdong Medical College (STIF201112) and thanks for Prof. P. Liu. TAS acknowledges the Brazilian funding agencies FACEPE and CNPq, and Ng also thank the University of Malaya (UM.C/625/1/HIR/247).

References:

(1) J. D. Rocca, D. M. Liu and W. B. Lin, *Acc. Chem. Res*. 2011, **44**, 957; (b) J. L. C. Rowsell and O. M. Yaghi, *Angew. Chem., Int. Ed*. 2005, **44**, 4670; (c) J. R. Li, R. J. Kuppler and H. C. Zhou, *Chem. Soc. Rev*. 2009, **38**, 1477.

(2) (a) P. S. Nugent, V. L. Rhodus, T. Pham, K. Forrest, L. Wojtas, B. Space and M. J. Zaworotko, *J. Am. Chem. Soc*. 2013, **135**, 10950; (b) B. L. Chen, S. C. Xiang and G. D. Qian, *Acc. Chem. Res*. 2010, **43**, 1115.

(3) C. Serre, F. Millange, C. Thouvenot, M. Noguès, G. Marsolier, D. Louër and G. Férey, *J. Am. Chem. Soc.* 2002, **124**, 13519; (b) C. Serre, C. Mellot-Draznieks, S. Surblé, N. Audebrand, Y. Filinchuk and G. Férey, *Science* 2007, **315**, 1828; (c) C. Mellot-Draznieks, C. Serre, S. Surblé, N. Audebrand and G. Férey, *J. Am. Chem. Soc.* 2005, **127**, 16273; (d) P. Horcajada, C. Serre, G. Maurin, N. A. Ramsahye, F. Balas, M. Vallet-Regí, M. Sebban, F. Taulelle and G. Férey, *J. Am. Chem. Soc*. 2008, **130**, 6774.

(4) C. Y. Sun, C. Qin, X. L. Wang, G. S. Yang, K. Z. Shao, Y. Q. Lan, Z. M. Su, P. Huang, C. G. Wang and E. B. Wang, *Dalton Trans*., 2012, **41**, 6906.

(5) (a) H. N. Wang, X. Meng, G. S. Yang, X. L. Wang, K. Z. Shao, Z. M. Su and C. G. Wang, *Chem. Commun*., 2011, **47**, 7128; (b) K. M. L. J. D. Rocca, Z. G. Xie, S. Tran and W. B. Lin, *J. Am. Chem. Soc*., 2009, **131**, 14261

(6) D. Zhao, W. S. Tan, D. Q. Yuan, W. G. Lu, Y. H. Rezenom, H. L. Jiang, L. Q. Wang and H. C. Zhou, *Adv. Mater*., 2011, **23**, 90.

(7) P. Horcajada1, T. Chalati, C. Serre, B. Gillet, C. Sebrie, T. Baati, J. F. Eubank, D. Heurtaux, P. Clayette, C. Kreuz, J. S. Chang, Y. K. Hwang, V. Marsaud, P. N. Bories, L. Cynober, S. Gil, G. Férey, P. Couvreur and R. Gref, *Nat. Mater*., 2010, **9**, 172.

(8) A. C. McKinlay, R. E. Morris, P. Horcajada, G. Férey, R. Gref, P. Couvreur and C. Serre, *Angew. Chem., Int. Ed*., 2010, **49**, 6260.

(9) Z. B. Ma and B. Moulton, *Coord. Chem. Rev*., **2011**, *255*, 1623.

(10) C. Y. Sun, C. Qin, C. G. Wang, Z. M. Su, S. Wang, X. L. Wang, G. S. Yang, K. Z. Shao, Y. Q.

Lan and E. B. Wang, *Adv. Mater*., 2011, **23**, 5629.

(11) A. Lam and A. Rivera, *Microporous Mesoporous Mater.* 2006, **91**, 181.

(12) X. L. Wang, C. Qin, E. B. Wang and Z. M. Su, *Chem. -Eur. J*., 2006, **12**, 2680.

(13) (a) J. Q. Liu, Y. Y. Wang, P. Liu, Z. Dong, Q. Z. Shi and S. R. Batten, *CrystEngComm*, 2009, **11**, 207; (b) J. Q. Liu, Y. Y. Wang, Y.N. Zhang, P.Liu, Q. Z. Shi and S. R. Batten, *Eur. J. Inorg. Chem*., 2009, 147; (c) J. Q. Liu, Y. Y. Wang and Z. B.Jia *Inorg. Chem. Commun*., 2011, **14**, 519; (d) J. Q. Liu, Y. Y. Wang and Y. S. Huang, *CrystEngComm*, 2011, **13**, 3733; (e) J. Wu, J. Q. Liu, G. Z. Ping, D. H. Xu and S. Hiroshi, *Inorg. Chem. Commun*., **2012**, *25*, 10; (f) P.M. Forster, N. Stock and A.K. Cheetham, *Angew. Chem. Int. Ed*., 2005, **44**, 7608; (g) P.M. Forster, A.R. Burbank, C. Ligage, G. Férey and A. K. Cheetham, *Chem. Comm*., 2004, 368.

(14) B. Lippert and P. J. Miguel, *Chem. Soc. Rev*., **2011**, *40*, 4475.

(15) G. M. Sheldrick, *SHELXL-97*: program for structure determination and Refinement: University of Göttingen: Göttingen, 1997.

(16) G. M. Sheldrick, SADABS 2.05; University of Göttingen: Germany, 2002.

(17) G. M. Morris R. , Huey, W. Lindstrom, M. F. Sanner, R. K. Belew, D. S. Goodsell and A. J. Olson, *J. Comp. Chem*., 2009, **30**, 2785

(18) R. Huey, G. M. Morris, A. J. Olson and D. S. Goodsell, *J. Comp. Chem*. 2007, **28**, 1145; (c) P. J. Goodford, *J. Med. Chem*., 1985, **28**, 849

(19) S. J. Weiner, P. A. Kollman, D. A. Case, U. C. Singh, C. Ghio, G. Alagona, S. Profeta and P. K. Weiner, *J. Am. Chem. Soc*., **1984**, *106*, 765.

(20) T. A. Soares, D. S. Goodsell, J. M. Briggs, R. Ferreira and A. Olson, J. *Biopolymers,* 1999, **50***,* 319; (21) T. A. Soares, R. D. Lins, T. P. Straatsma and J. Briggs,M. *Biopolymers,* 2002, **65**, 313.

(21) M. O. Rodrigues, M. V. de Paula, K. A. Wanderley, I. B. Vasconcelos, S. Alve and, T. A. Soares, *Inter. J. Quantum Chem*., 2012, **112**, 3346.

(22) I. B. Vasconcelos, T. G. da Silva, G. C. G. Militão, T. A. Soares, N. M. Rodrigues, M. O. Rodrigues, N. B. da Costa, R. O. Freire and S. Alves, *RCS Adv*., 2012, **2**, 9437.

(23) V.A. Blatov, A.P. Shevchenko and D.M. Proserpio, *Cryst. Growth Des*. 2014, **14**, 3576.

(24) M. Li, D. Li, M. O'Keeffe and O. M. Yaghi, *Chem. Rev*. 2014, **114**, 1343.

(25) (a) M. E. Lines, *J. Phys. Chem., Solids,* 1970, **31**, 101; (b) Q. Yu, X. Q. Zhang, H. D. Bian, H. Liang, B. Zhao, S. P. Yan and D. Z. Liao, *Cryst. Growth & Des*., 2008, **8**, 1140; (c) S. R. Breeze, S. Wang, J. E. Greedan and N. P. Raju, *J. Chem. Soc., Dalton Trans*., 1998, 2327; (d) S. Mukhopadhyay, P. B. Chatterjee, D. Mandal, G. Mostafa, A. Caneschi, J. V. Slageren, T. J. R. Weakley and M. Chaudhury, *Inorg. Chem*., 2004, **43**, 3413; (e) R. L. Carlin, K. Kopinga, O. Kahn and M. Verdaguer, Inorg. Chem., 1986, 25, 1786; (f) P. R. Levstein and R. Galvo, *Inorg. Chem*., 1990, **29**, 1581; (g) E. Ruiz, P. Alemany, S. Alvarez and J. Cano, *Inorg. Chem*., 1997, **36**, 3683; (h) J. P. Malrieu, R. Caballol, C. J. Calzado, C. D. Graaf and N. Guihéry, Chem. Rev., 2014, 114, 429; (i) X. L. Qi, C. Zhang, B. Y.

Wang, W. Xue, C. T. He, S. Y. Liu, W. X. Zhang and X. M. Chen, *CrystEngComm*, 2013, **15**, 9530; (j) J. H Van Vleck, Electric and Magnetic Susceptibilities, Oxford University Press, London, 1932; (k) W. Barros, B. C. da Silva, N. V. Reis, C. L. M. Pereira, A. C. Dorquetto, J. Cano, K. R. Piorota, E. F. Pedroso, M. Julve and H. O. Stumpf, *Dalton Trans*., 2014, DOI:10.1039/C4DT01180E; (m) F. Mroziński, A. Tomkiewicz, M. Nahorska and B. Korybut-Daskiewicz, *Mater. Sci*., 2003, **21**, 161.

(26) (a) S. S. Nagarkar, A. K. Chaudhari and S. K. Ghosh, *Inorg. Chem*. 2012, **51**, 572; (b) B. Liu, J. T. Shi, K F. Yue, D. S. Li and Y. Y. Wang, *Cyrst. Growth Des*. 2014, **14**, 2003; (c) L. Du, Z. Lu, K. Zheng, J. Wang, X. Zheng, Y. Pan, X. You, J. Bai, *J. Am. Chem. Soc*., 2013, **135**, 562; (d) S. Furukawa, Y. Sakata and S. Kitagawa, *Chem. Lett*., 2013, **42**, 570; (e) R. Kitaura, K. Seki, G. Akiyama and S. Kitagawa, *Angew. Chem. Int. Ed.,* 2003, **42**, 428*;* (f) T. K. Maji, R. Matsuda and S. Kitagawa, *Nat. Mater*., 2007, **6**, 142.

(27) (a) M. L. Connolly, *Science,* 1983, **221**. 709; (b) C. Daiguebonne, N. Kerbellec, K. Bernot, Y. Gérault, A. Deluzet and O. Guillou, *Inorg. Chem.* 2006, **45**, 5399; (c) Y. C. Qiu, H. Deng, S. Yang, J. Mou, C. Daiguebonne, N. Kerbellec, O. Guillou and S. R. Batten, *Inorg. Chem.,* 2009, **48**, 3976; (d) N. Kerbellec, C. Daiguebonne, K. Bernot, O. Guillou and Guillou, Le X. *J. Alls.Comp.* 2008, **451**, 377; (e) N. Rosi, J. Kim, M. Eddaoudi, B. Chen, M. O'Keeffe and O. M. Yaghi, *J. Am. Chem. Soc*., 2005, **127**, 1504.

(28) P. Horcajada, C. Serre, M. Vallet-Regi, M. Sebban, F. Taulelle and G. Férey, *Angew. Chem.* 2006 , **118** , 6120 ; *Angew. Chem. Int. Ed.,* 2006, **45**, 5974 .

(29) X. Huang and C. S. Brazel, J. Control. Release, 2001, **73**, 121.

Table 1 the crystallographic data of **1**–**2**.

Complex	**1**	**2**
Empirical formula	$C_{28}H_{24.5}CuN_{3.5}O_5$	$C_{25}H_{28}CuN_2O_9$
Formula mass	553.55	564.03
Crystal system	monoclinic	monoclinic
Space group	$P2_1/c$	$C2/c$
a [Å]	13.7894(11)	13.7352(16)
b [Å]	17.4839(14)	17.888(2)
c [Å]	10.8445(9)	11.0251(14)
α [°]	90	90
β [°]	100.429(1)	100.460(2)
γ [°]	90	90
V [Å^3]	2571.3(4)	2663.7(6)
Z	4	4
d_{calcd} [g·cm^{-3}]	1.430	1.406
μ [mm^{-1}]	0.894	0.873
F(000)	1144	1172
Reflections/unique	15587/3356	7680/1602
R(int)	0.0329	0.0821
R_1, wR_2 [$I>2\sigma(I)$]	0.0377, 0.0964	0.0592, 0.1711
R_1, wR_2 (all data)	0.0654, 0.1104	0.1104 , 0.1955

Table 2. Selected bond distances (Å) and angles (°)

		1	
Cu1–O1	1.925(8)	Cu1–O3	1.928(4)
Cu1– N1	2.039(6)	Cu1–N2	2.044(7)
Cu1–O1W	2.321(8)	O3–Cu1–O1	175.1(8)
O1 –Cu1 –N1	89.9(7)	O2–Cu1–N1	90.8(7)
N1– Cu1– O1W	100.5(3)	N2–Cu1–O1W	90.2(7)
		2	
Cu1–O1#1	2.009(3)	Cu1–N1#1	2.085(4)
Cu1–O1W	2.257(13)	N1–Cu1–N1	161.81(6)
O1 –Cu1 –O1#1	160.93(7)	O1–Cu1–N1	88.53(14)

#1: -x+2, -y, -z+1.

Two isoreticular metal–organic frameworks with $CdSO_4$-like topology: selective gas sorption and drug delivery

Jian-Qiang Liu[a*], Jian Wu[b], Zhen-Bin Jia[a], Hong-Lang Chen[a], Qin-Lin Li[a], Hiroshi Sakiyama[c], Thereza A. Soares[d*], Ren-Fei[e]* Carole Daiguebonne[f], Olivier Guillou[f*], Ng, Seik Weng[g]

All Figures

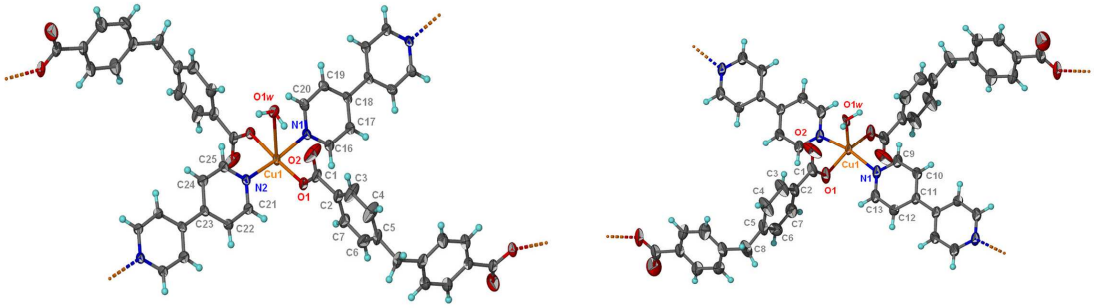

Fig. 1 (a) Coordination environment of Cu(II) in **1** and (b) Coordination environment of Cu(II) in **2.**

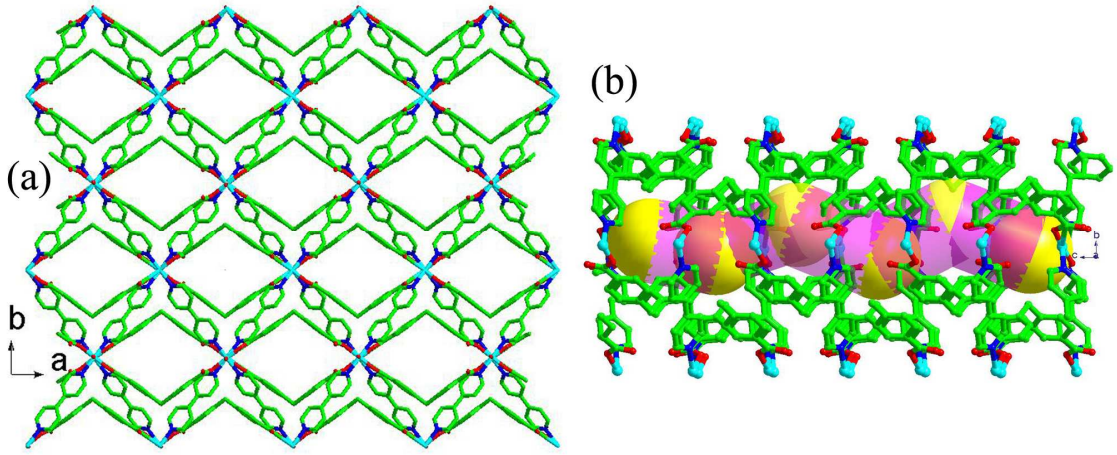

Fig.2 (a) view of the 3D framework in **1** and (b) perspective view of 1D channel in **1**.

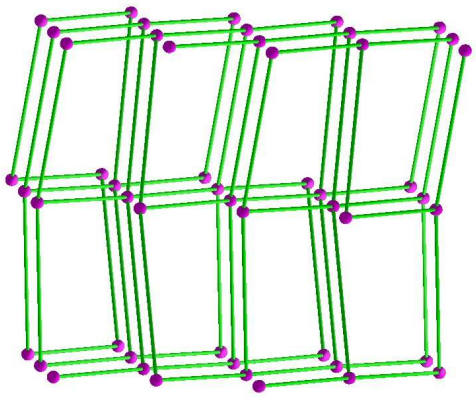

Fig. 3 perspective view of **$CdSO_4$**-like topology

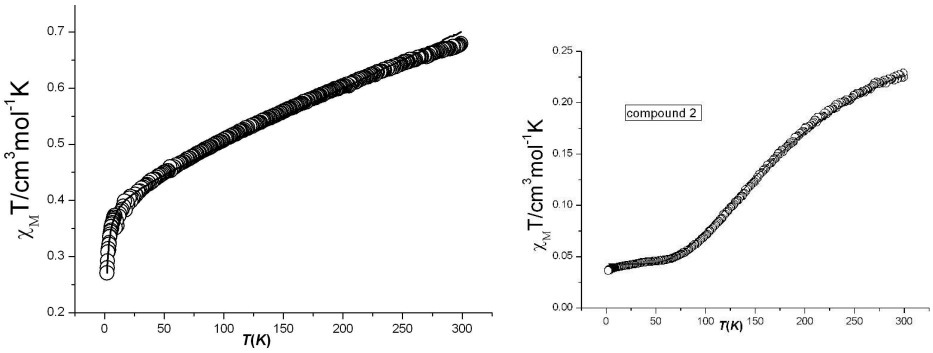

Fig. 4 (a) Plots $\chi_M T$, versus T for **1** (left) and (b) plots $\chi_M T$ versus T for **2** (right), solid lines represent fits to the data.

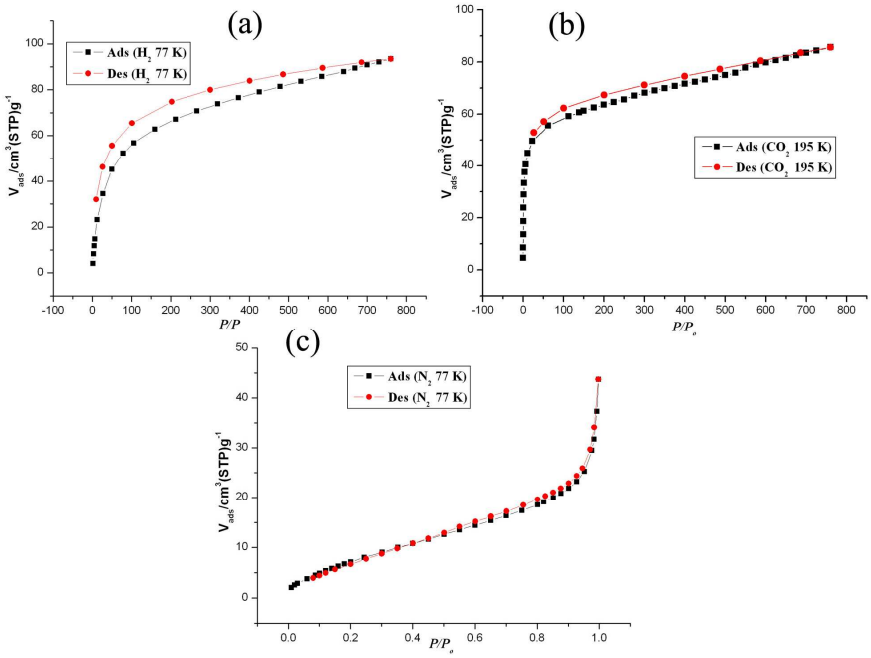

Fig. 5 Gas adsorption isotherms of **1**: CO2 (195 K), H2 (77 K) and N2 (77 K) (filled symbols,

adsorption; open symbols, desorption).

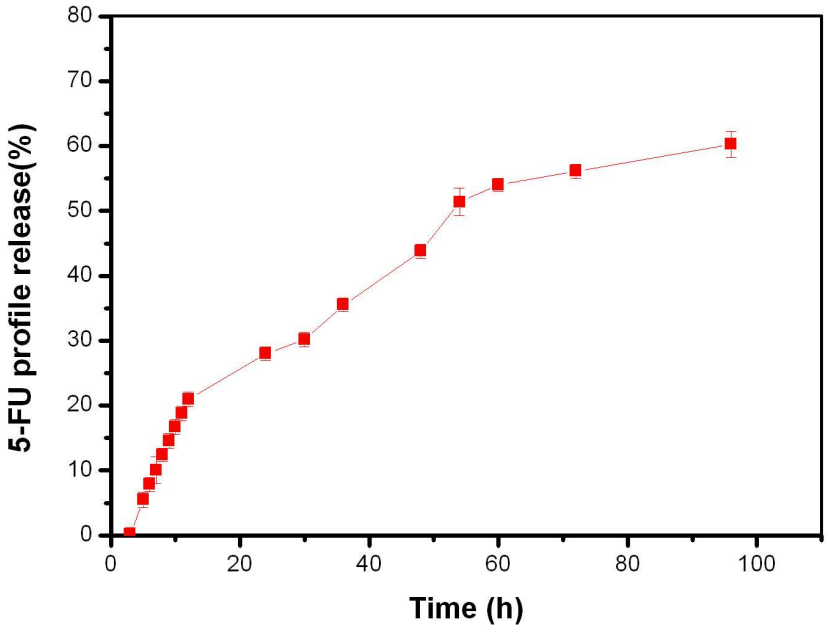

Fig. 6 the release process of 5-FU from the drug-loaded **1** (% 5-FU vs. time).

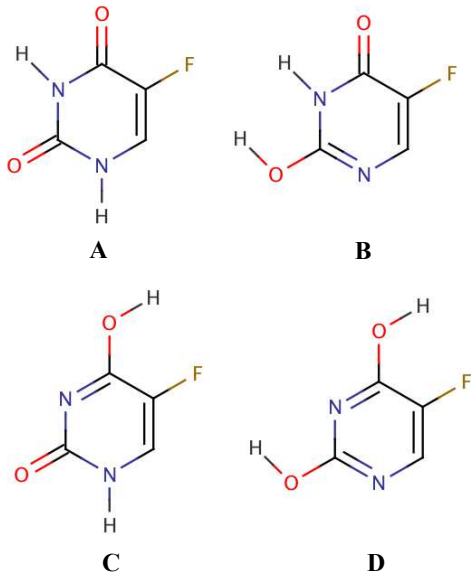

Fig. 7 Tautomeric forms of 5-fluorouracil (*J. Phys. Chem. A*, 2005, 109, 1981): A) 2,4-dioxo (diketo form), B) 2-hydroxy-4-oxo (keto–enol form), C) 2-hydroxy-4-oxo (keto–enol form), and D) the 2-hydroxy-4-hydroxy (dienol form).

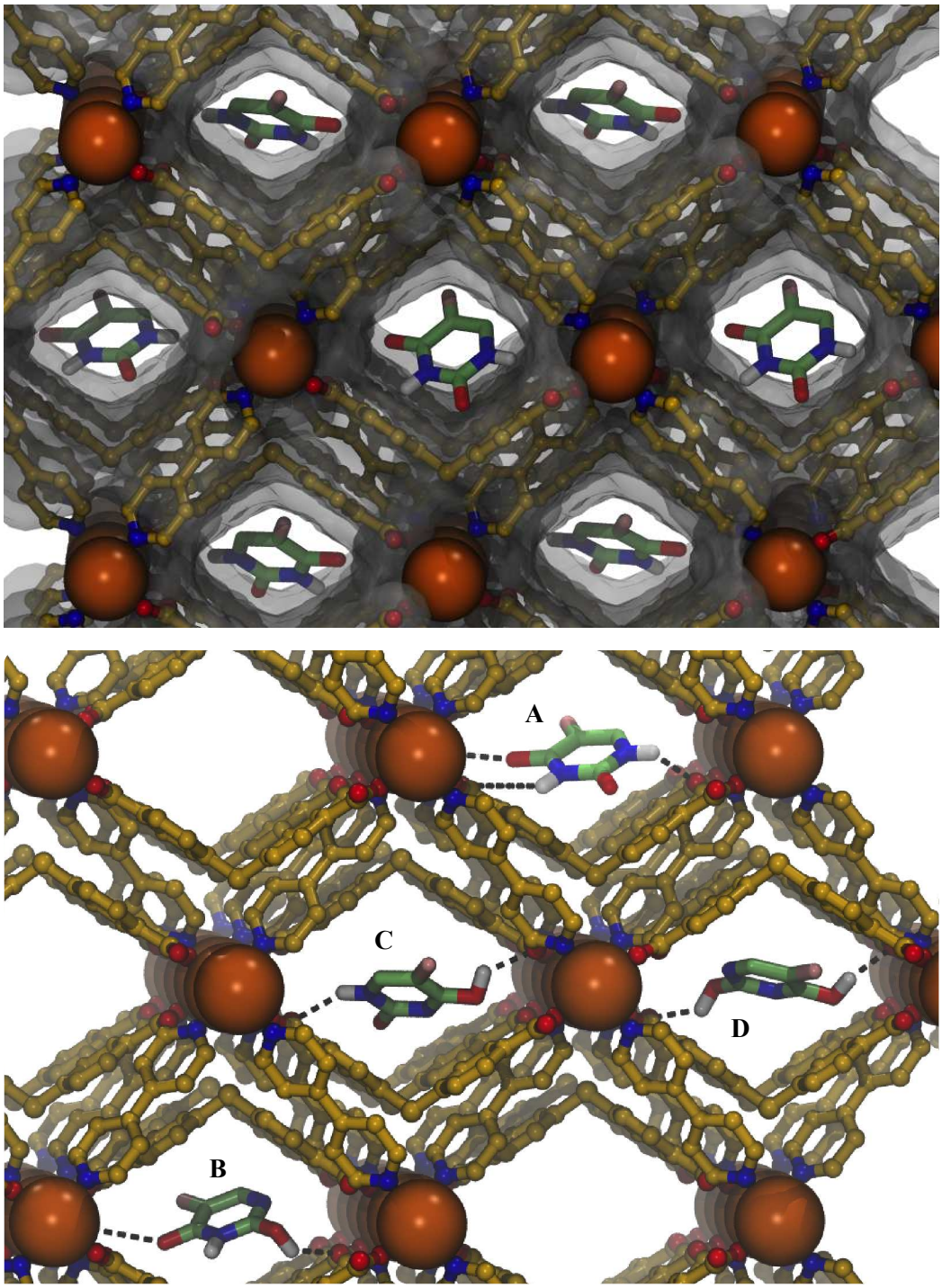

Fig. 8 Predicted conformation of 5-fluorourcil upon binding to metal-organic framework **1**. Top: Representation of the main diketo tautomer bound to the inner space of the pore defined by molecular (van der Waals) surface of the framework. Bottom: Predicted conformations of 5-fluorourcil tautomers upon binding to framework **2**. Tautomeric forms are A) diketo, (B-C) keto–enol, and D) dienol (see Figure 7 for detailed chemical structures). Dash-lines represent hydrogen bond or short-distance electrostatic interactions between polar or charged groups in the drug

and in the framework.

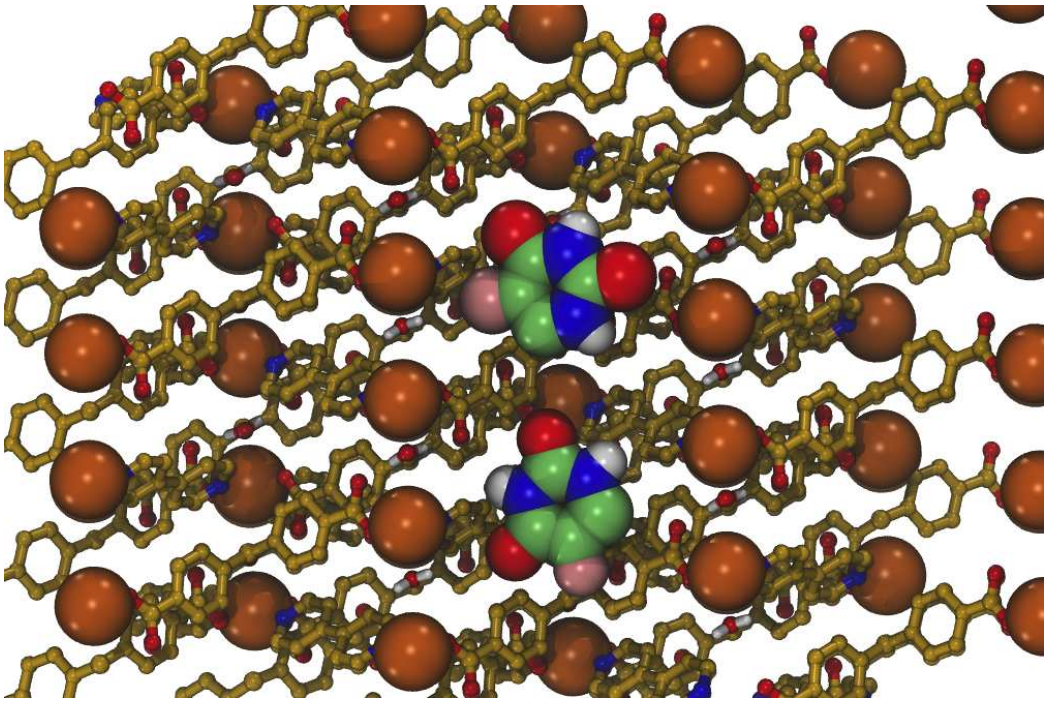

Fig. 9 Predicted conformation of 5-fluorourcil upon binding to metal-organic framework **1** containing a second copy of the drug. 5-fluorourcil is represented in its diketo form. This view was obtained through the rotation of the system in 90 degrees towards the reader from the view in Figure 8. Atoms on the top of the pore were removed for clarity.

Two isoreticular metal–organic frameworks with $CdSO_4$-like topology: selective gas sorption and drug delivery

Jian-Qiang Liu[a*], Jian Wu[b], Zhen-Bin Jia[a], Hong-Lang Chen[a], Qin-Lin Li[a], Hiroshi Sakiyama[c], Thereza A. Soares[d*], Ren-Fei[e]* Carole Daiguebonne[f], Olivier Guillou[f*], Ng, Seik Weng[g]

The present work reports on two isoreticular metal–organic frameworks. The drug load and release capacity of these MOFs were evaluated using the anticancer drug 5-fluorouracil (5-FU) as a model. We have also investigated the binding mode of 5-FU to these frameworks, which provides an atom-level view of host-guest interactions.